Distribution Category:
LMFBR Safety (UC-79p)

ANL-75-12

ARGONNE NATIONAL LABORATORY
9700 South Cass Avenue
Argonne, Illinois 60439

POSTACCIDENT HEAT REMOVAL: LARGE-SCALE MOLTEN-FUEL-SODIUM INTERACTION EXPERIMENTS

by

T. R. Johnson, J. R. Pavlik, and L. Baker, Jr.

Reactor Analysis and Safety Division

February 1975

TABLE OF CONTENTS

BLANK PAGE

LIST OF FIGURES

LIST OF TABLES

converted to particulate, even though the initial sodium depth was only about 4 in. The results showed that it requires an almost equal weight of fuel to sodium in a sodium depth of 4 in. before the conversion to particulate is incomplete. Thus it is expected in many hypothetical accident situations where molten fuel must move through many feet of sodium that the molten fuel will be completely converted to particulate.

The large pieces which were recovered from one run and which comprised about 10% of the total material had void volumes greater than 20% and void volumes connected to the surface of greater than 15%. With this exception, the recovered particles of UO_2 and metal alloy had size distributions that were generally in the range of particle sizes from earlier in-pile and small-scale laboratory tests. The metal particles were larger on the average than the oxide particles.

Most of the recovered particles were angular, with a small proportion of spherical or smooth particles. Under the conditions of these tests (large mass of UO_2 injected at a relatively low velocity into quiescent sodium), the final particles were probably the result of fracturing of larger solidified or partially solidified particles by thermal shock. Fragmentation during the interaction apparently occurred over a period of time of the order of 1 second.

III. EXPERIMENTAL APPARATUS AND PROCEDURE

The apparatus and the thermite techniques employed in these experiments were described in detail in an earlier report.[1] The interaction apparatus consisted of a sodium-filled crucible contained in an 18-in.-dia pressure vessel (see Fig. 1) with the uranium metal-MoO_3-CrO_3 mixture charged to a reaction chamber (see Fig. 2) bolted to the top cover plate of the pressure vessel. The assembled apparatus is shown in Fig. 3 with the spring-loaded vessel cover in place. The interaction vessel was designed to contain static pressures of 250 psig safely and to release gas through the spring-loaded vessel cover at pressures of approximately 100 psig, and through a 200 psi rupture disk. The apparatus was located in a decontaminated hot cell that was capable of containing any credible release from the interaction vessel.

A. Characteristics of Thermite-produced UO_2

The thermite reactant mixture had a mole ratio of 1.0 U:5/9 MoO_3:1/9 CrO_3. The calculated adiabatic temperature of this composition at 1 atm was 6200°F, which was limited by the boiling point of UO_2. The heat of reaction was sufficient to boil all of the chromium metal produced. References in this report to the UO_2 produced by the thermite reaction imply an intimate mixture of 83 wt% UO_2 and 17 wt% Mo. In an earlier report[2] describing the thermite technique for producing UO_2, the measured temperatures of the product were in the range from 5250 to 5600°F. More recent measurements have indicated that molten UO_2 produced for the large-scale interaction experiments had temperatures up to 5800°F. For the calculations in this report, it was assumed that the average temperature of the UO_2 entering the sodium was 5700°F, with an enthalpy of 670 Btu/lb, and that all of the chromium had been vaporized. This temperature was based

BLANK PAGE

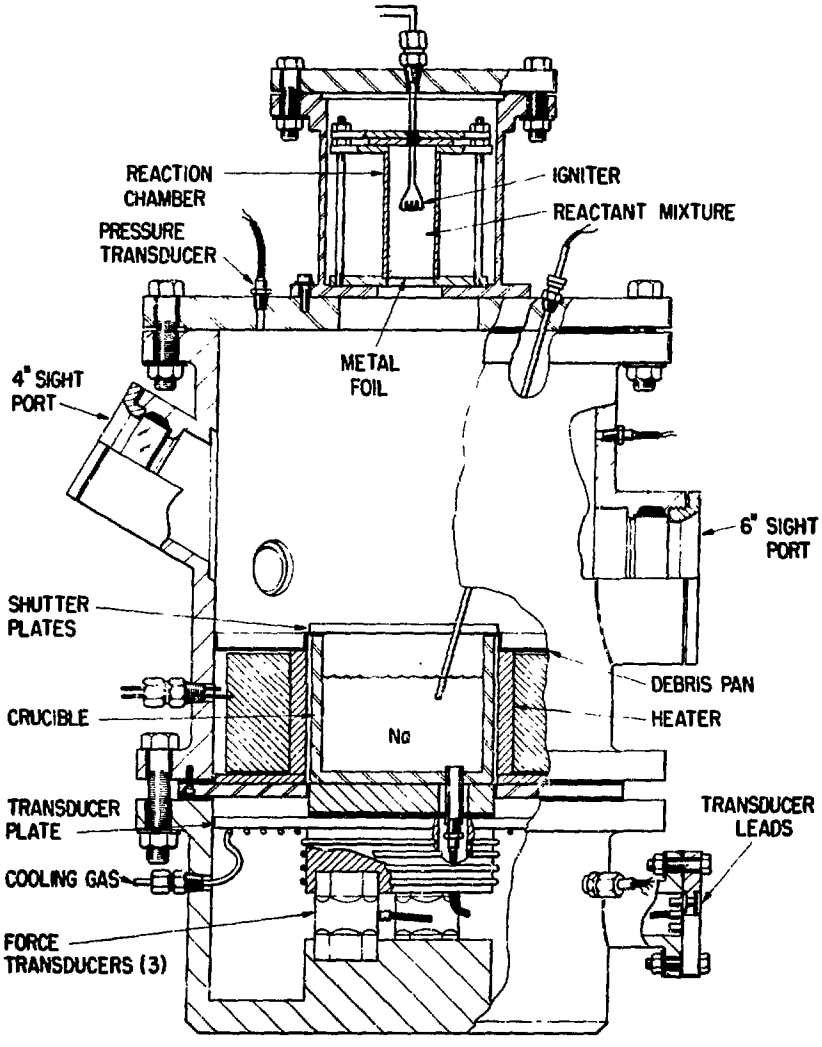

Fig. 1. Interaction Vessel Assembly. ANL Neg. No. 900-1914.

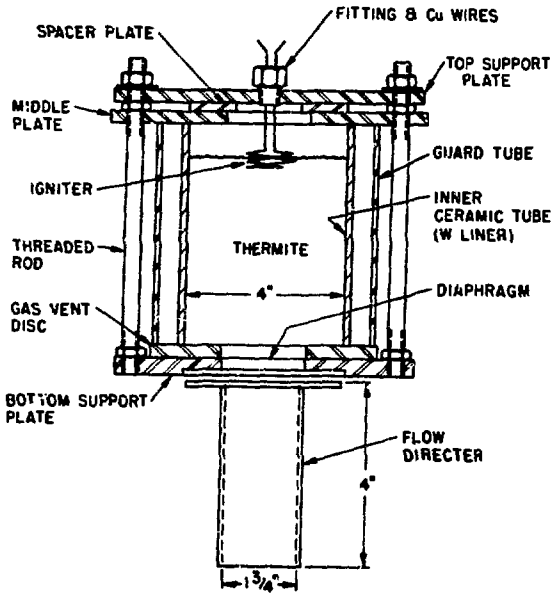

Fig. 2. Inner Reaction Chamber.

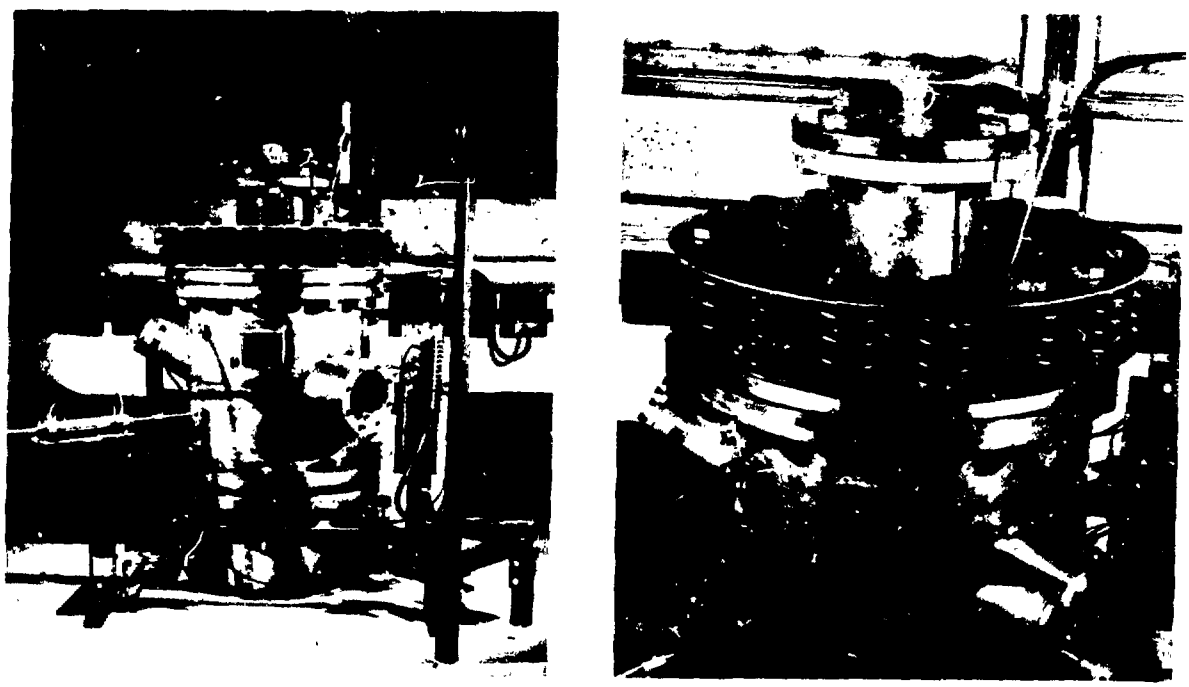

Fig. 3. Photographs of Assembled Interaction Vessel.

on the calculated adiabatic temperature and estimated heat losses from the reaction products to the reaction chamber and to the atmosphere of the interaction vessel.

The form of the molten material entering the sodium was judged to be a stream of fairly closely spaced drops with dimensions of the order of a centimeter. The stream could not be characterized as a two-phase jet of liquid and gas. Motion pictures of earlier small-scale experiments had shown that 100- to 300-g charges were released as liquid drops about 0.5 cm in diameter, which was the approximate size of the release orifice. These falling drops tended to stretch and break in a fashion typical of large, liquid drops.

Attempts were made to take high-speed motion pictures of the falling UO_2 stream and the interaction events through the two sight ports in the interaction vessel, but smoke and dust from the thermite reaction completely obscured the pictures in all but one of the three interaction runs (M2) and in a large-scale (6 lb) UO_2 release into a dry crucible. (The latter run is reported separately.[7]) Individual liquid drops could not be discerned on these motion pictures, but the initial front of hot material and the bulk liquid stream could be identified. The pictures showed that the liquid UO_2 fell vertically with velocities between 30 and 60 ft/sec, and was not sprayed with any significant horizontal component. This observation was supported by the fact that in run M1 a maximum of 5 g of UO_2 was found outside the sodium crucible.

B. Instrumentation

The gas-phase pressure in the interaction vessel was measured by piezoelectric transducers (Kistler Model 607C1) located in the top cover plate and side wall. A similar transducer in the bottom of the crucible measured pressures in the liquid sodium. This transducer was attached to a 0.54-in.-ID downleg at least 2 in. below the crucible in a cooled region of the transducer housing because the maximum operating temperature of the transducer was 260°F. The procedure used to fill the crucible containing sodium insured that the downleg was completely filled with sodium, and thermocouples were attached to the downleg and transducer to insure proper temperatures for the interaction event. The crucible rested on three force transducers (Kistler Model 937A) that measured the downward forces created by the interaction event. Since one transducer could not accurately measure the full range of possible forces, a different amplification was used for each force transducer to monitor forces from 10 to 10,000 lb. During an experiment, the signals from the six transducers were recorded on magnetic tape and on an oscillograph. The data on tape were later recorded on the oscillograph with a time expansion of 16 to 1. The frequency response of this instrumentation was limited by the tape recorder to approximately 20 kHz.

Before and after each run, all transducers were calibrated and the calibration signals recorded on the same magnetic tape as the experimental data. The two calibrations agreed within 10% in all cases.

C. Procedure

Before each experiment, the vessel was cleaned and then degassed under vacuum at 1100°F. For this operation, the interaction vessel was assembled without transducers; there was no sodium in the crucible or thermite in the reaction chamber. After degassing, the crucible and reaction chamber were removed and placed in an argon-atmosphere glovebox, where the transducer was attached to the crucible. Liquid sodium was poured into the crucible, insuring that the downleg was completely filled, and then allowed to freeze. After reassembling the vessel with all transducers and the sodium-filled crucible in place but without the reaction chamber, the vessel was filled with argon, leak tested, and the instrument circuits were checked. The chamber was charged in the glovebox with the thermite reactant mixture and then bolted to the top cover of the interaction vessel. After the sodium had been heated to the proper temperature, the instrumentation to record the pressures and forces was turned on, pneumatic cylinders were actuated to withdraw the shutters over the crucible and the thermocouple well in the sodium, and the sodium heaters were turned off. The thermite reaction was started near the top of the powders by an electrically heated wire, and the reaction front progressed through the solids in less than 1 sec. Gas pressure resulting from heating the argon in the chamber and from the gases generated by the reaction was released through slots in the gas-vent disc at the bottom of the chamber. When the igniter wire had broken, indicating that the thermite reaction had started, the electrical power to the igniter was turned off automatically to eliminate a serious source of electrical noise, the motion-picture cameras were started, and a timing mark was recorded on the data record. After an additional 1-2 sec after ignition, gravity and gas pressure caused the molten reaction products to be ejected downward through the melting metal foil in the bottom of the chamber. As soon as possible after the interaction, the pneumatic cylinders were manually actuated to reinsert the thermocouple in the sodium and to close the shutters.

IV. EXPERIMENTAL RESULTS

The experimental conditions and a few general results for the three interaction experiments are listed in Table I. The force and pressure records shown in Figs. 4, 5, and 6 include indications of the times of ignition, as well as UO_2 release and fall from the reactor and entry into the sodium. For times beyond those shown, the sodium pressure and force signals returned uniformly to their initial values. The magnitudes of the liquid-phase pressure pulses and the associated force pulses from run M3 are listed in Table II.

Motion pictures of the sequence of events could not be obtained. Therefore, the timing of the events had to be inferred from the pressure and force data and from earlier experiments in which the rate of reaction had been measured and motion pictures of the released materials had been obtained. Immediately after ignition, hot gases from the reaction chamber caused the pressure in the interaction vessel to increase rapidly by 4 to 8 psi. Pressure and force measurements made before and for a few milliseconds after ignition were severely obscured by a large 60-Hz noise signal from the current to the igniter wire. After this initial gas release, the

Table I. Experimental Conditions and Results for Large-scale UO_2-Sodium Interactions

RUN #	M1	M2	M3
Conditions			
Quantity UO_2-Mo-Cr Released (lb)	1.4	6.8	3.0
Quantity Sodium (lb)	6.6	7.1	6.5
Temperature of Sodium (°F)	550	570	1160
Vessel Pressure at Entry (psia)	50	56	26
Estimated Entry Velocity (ft/sec)	11[1]	60[2]	13[1]
Calculated Adiabatic Temperature[3] (°F)	1170	2160	1960
Results			
Final Sodium Temperature (maximum measured) (°F)	740[4]	1300[5]	1450[4]
Maximum Vessel Pressure (psia)	62	100[6]	(>40[7] < 100)
Sodium Ejected from Crucible (lb)	0.02	5.0	4.6
UO_2-Mo-Cr Ejected from Crucible (lb)	0.01	1.33	1.21
Average Particle Size of UO_2-Mo-Cr			
- total material (μm)	510	220[8]	170
- material in crucible (μm)	510	300[8]	200
- ejected material (μm)	-	140	180

1. Velocity calculated from time of fall.
2. Velocity estimated from motion pictures.
3. Assumed no boiling of sodium and thermite enthalpy = 670 Btu/lb.
4. Temperature from thermocouple under crucible.
5. Temperature from immersion thermocouple.
6. Vessel cover opened about 90 psia.
7. Vessel pressure at time of transducer failure.
8. Not including large porous pieces.

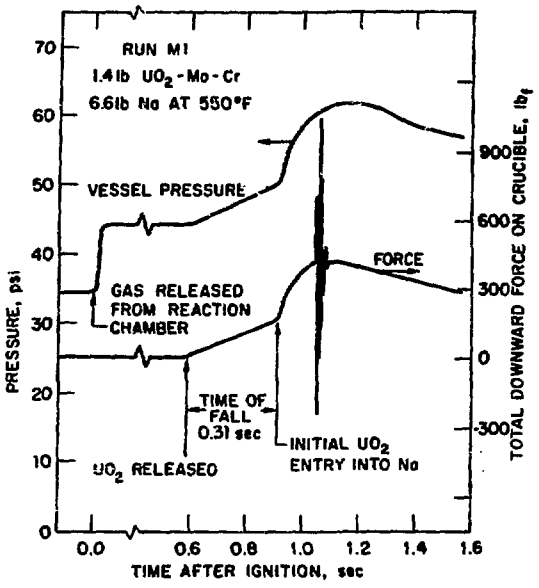

Fig. 4.
Experimental Measurements from Large-scale UO_2-Na Interaction Test M1.

Fig. 5.
Experimental Measurements from Large-scale UO_2-Na Interaction Test M2.

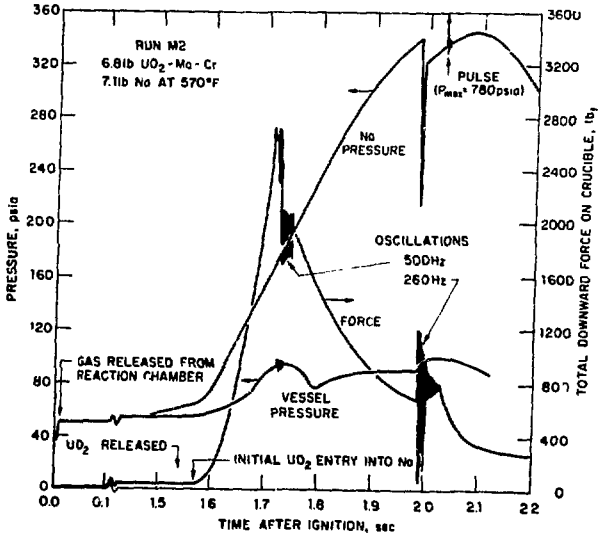

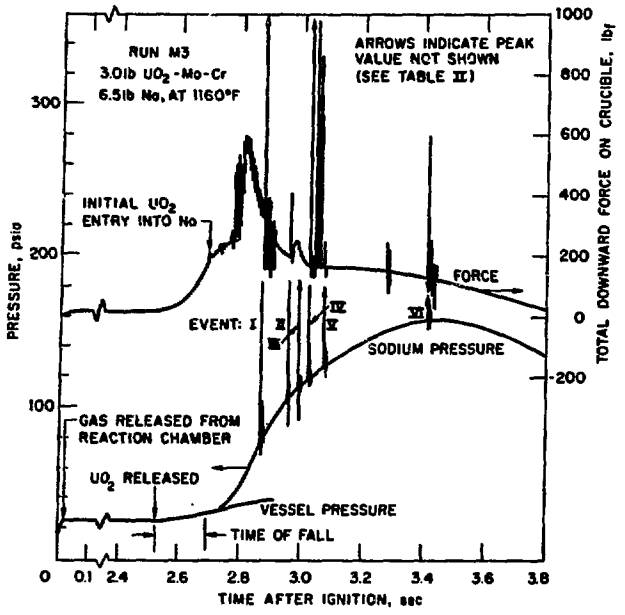

Fig. 6.
Experimental Measurements from Large-scale UO_2-Na Interaction Test M3.

Table II. Sharp Pressure-force Events from Run M3

Event No.	Measured Peak Pressure		Measured Peak Force Above Background (lb_f)	Impulse (First Force Pulse) (lb_f-sec)
	Absolute (psia)	Above Background (psi)		
I	180	100	780	1.2
II	180	80	220	0.4
III	350	240	150(1)	-
IV	330	220	2500	4.4
V	430	300	60	0.1
VI	240	70	460	0.7

(1) Broad force pulse with a rise time to half height of about 3 msec. Not coincident with pressure pulse.

reaction was completed in less than 1 sec; the molten reaction products remained in the reaction chamber for a longer period as the metal diaphragm was melting. During this period, the vessel pressure remained relatively constant. The release of molten materials into the interaction vessel was marked by a small, linear pressure rise (about 20 psi/sec) due primarily to the radiant heating of the vessel atmosphere by the falling UO_2. This rate of pressure increase was roughly equal to that calculated to result from radiant heat transfer from the molten stream. In runs M1 and M3, the velocity of entry into the sodium was estimated from the duration of this linear pressure change, which was assumed to be the time to fall from the reaction chamber to the sodium surface. The entry velocity for M2 was measured on motion pictures of the release. The entry of molten materials into the sodium was marked first by a rapid, nonlinear increase in the vessel pressure and then after several hundredths of a second by a rapidly increasing sodium pressure.

In general, the measurements of the vessel pressure by the transducers mounted in the vessel cover and side wall appeared to have a precision and accuracy well within $\pm$10% of full scale. The pressure measurements could be associated with interaction events up to the time when the transducer diaphragm was struck by hot materials, causing a sudden indication of an apparent large negative pressure. This behavior is typical of piezoelectric transducers of the type used in these experiments.

Similar accuracy and precision applied to the force and sodium pressure transducers. Although the pulses in the sodium pressures and crucible forces could be associated reasonably with events occurring during the interactions, the longer, smoother background liquid pressures and crucible forces could not be related to credible interaction events. It was thought that the large forces on the crucible were caused by a small difference in pressure between the upper and lower sections of the vessel. In runs M1 and M3, the vessel pressure and force curves initially had the same general shape. A partial seal could have been formed between the vessel side wall, sodium pans, and sodium crucible. A differential pressure of 2 psi applied over the entire cross section of the vessel would have resulted in a force of 1000 lb on the crucible supports.

The pressure transducer mounted under the crucible indicated the sodium pressure inside the crucible relative to the pressure at the time it was last grounded, that is, relative to the vessel pressure before ignition of the thermite. The cause of the high sodium pressures, which persisted for several tenths of a second in runs M2 and M3, was not understood, but the likely cause was entrapment of sodium and a few hot UO_2 particles in the downleg. In run M2, a semisolid layer of UO_2 was formed, possibly covering the entrance to the downleg, but in run M3 no such UO_2 layer was found after the run. It seemed improbable that the liquid-phase pressure signal could have been affected by either mechanical stresses or thermal effects. Sufficient heat could not have been conducted through the sodium in the downleg to raise the temperature of the transducer diaphragm and affect the signal. Calculations showed that a temperature of 5400°F applied at one end of the 2-in.-long sodium column (the length of the downleg used in M2) would raise the temperature of the sodium at the other end by less than 0.04°F after 0.4 sec. With the downleg at room temperature and either empty or half filled with water, pouring boiling water directly into the downleg caused

the typical anomalous indication of a large negative pressure. Stressing the crucible by applying a flame to the bottom for several seconds did not cause any noticeable deflection in the transducer signal. The transducer was mounted as recommended by the manufacturer to minimize stresses in the diaphragm caused by strains in the supporting structure. To establish firmly the cause of the sustained liquid-state pressure indications would require additional experimentation.

A. Experiment M1

Data were obtained from one of the two transducers measuring vessel pressure and from two of the three force transducers. The other transducers and the transducer in the sodium-filled crucible did not produce useful signals because either the amplification was too low or the instrument malfunctioned. From the large pressure rise immediately following ignition, it was estimated that the increased pressure due to the reaction was completely vented to the interaction vessel, and that the pressure of the chamber and vessel were nearly equal at the time of release. From this and from the duration of the linear rise in the gas pressure, which corresponded to the free-fall time for the 19 in. from the bottom of the reaction chamber to the sodium, it was inferred that the liquid UO_2 fell from the chamber with a very low initial velocity.

Because the shape of the force curve, except for the oscillations, was similar to the vessel-pressure curve, it was assumed that the smooth force response was due to a slight difference in pressure between the interaction vessel above and below the crucible. About 0.13 sec after entry, the crucible exerted an oscillatory force on its supports with a frequency of about 220 Hz. In the subsequent two runs, similar oscillating forces were found and apparently were initiated by rapidly rising pressure pulses in the liquid sodium. The frequency of 200-250 Hz seemed to be the typical response of the crucible-force transducer system to a sharp pressure pulse. When bags of sand were dropped into the crucible either when it was dry or filled with water, the system oscillated irregularly with a frequency between 20 and 30 Hz.

B. Experiment M2

Useful data were obtained from all six transducers in run M2, but a few hundred milliseconds after entry, the two pressure sensors on the vessel indicated large negative pressures, probably because they had been struck by hot sodium. Motion pictures of the falling UO_2 partly obscured by smoke and a small portion of the cloud of sodium vapor were obtained at a film speed of 2660 frames/sec. The velocity of the UO_2 falling from the reaction chamber was measured in the pictures to be roughly 60 ft/sec. This higher velocity may have been caused by high pressure in the reaction chamber, which resulted from incomplete venting of gases following the ignition. From timing marks placed on the film every 1.0 msec, the release of UO_2 from the chamber was found to begin 1.54 sec after ignition. If allowance is made for the time to fall into the crucible, this agrees within 0.01 sec with an entry time of 1.57 sec inferred from the records of the vessel pressure. The time from the beginning to the end of the release as seen on the film was judged to be 10 msec, which would be the time for the bulk of the UO_2 to enter the sodium. If the diameter of the

UO_2 stream was 1-5/8 in. (the inside diameter of the nozzle after allowing for the coating of solidified UO_2), the average density of the molten stream was 5.6 gm/cc. The stream of molten UO_2 appeared on the film to be dense, with no significant amounts of material being sprayed to the sides.

A small portion of the cloud of sodium vapor emanating from the crucible could be seen for 17 msec starting 1.60 sec after ignition. This does not imply that the vapor cloud started then, since most of the picture was obscured by dense smoke. The sodium vapor was not luminous as it had been in Armstrong's experiments,[4] but was illuminated by light from the reaction chamber. Dark streams and drops, probably cold sodium, were seen moving through the vapor at velocities between 10 and 20 ft/sec. From this observation of the cold sodium drops moving at relatively low speeds and the inference that a fairly dense mass of UO_2 entered the sodium, it seems likely that much of the sodium found outside of the crucible was splashed out rather than being thrown out by boiling sodium.

As sodium was vaporized, the vessel pressure rose to about 95 psia, causing the spring-loaded cover to open, releasing gas and vapor to the cell for approximately 400 msec. The pressure transducer in contact with the sodium indicated a gradually rising and unusually large pressure, which was interpreted to be the pressure of sodium trapped under UO_2 in the small downleg connecting the transducer to the bottom of the crucible. The negative spike in the sodium pressure may have been caused by a short-term venting of this trapped sodium or by the sudden closing of the vessel cover. This event initiated the force oscillations with a frequency of 260 Hz. Following the negative pressure pulse, there was a sharp positive pressure pulse that had a measured rise time of 40 μsec, which was equal to the maximum frequency response of the instrumentation. The indicated pressure of 780 psia (450 psi above the background sodium pressure) was the highest pressure recorded. The impulse of this pressure pulse was about 4 lb_f-sec. No evidence of any coincident pressure pulse in the vapor phase could be found, but the sensitivity of the pressure transducers would limit the detection of a gas-phase pulse propagated from a liquid-phase event.

The rapid increase in the crucible force to 2700 lb_f at 130 msec after the initial UO_2 entry was indicative of the stream of liquid UO_2 striking the crucible bottom at a velocity roughly equal to the entry velocity of 60 ft/sec. From the UO_2 debris found in the crucible, it appeared that molten UO_2 struck the crucible bottom near the center and splashed upward along the sides. When a 2-lb bag of sand was released into the dry crucible at velocities of 10 and 60 ft/sec, the total initial force pulses generated were 200 and 1500 lb_f, respectively, and the rise time of the initial pulses was roughly 5 msec. Close to the time the vessel cover first opened, the crucible force and the vessel pressure oscillated with a frequency of about 500 Hz, which may have been caused by vibrations of the vessel cover and springs or by the escaping gas flowing over the gasket ring of the vessel cover.

A total of 70% of the sodium was ejected from the crucible, with perhaps one-third of all sodium being physically splashed out by the entering UO_2. About 20% of the UO_2 was ejected from the crucible and of the UO_2

remaining in the crucible, about one-half had formed a fairly cohesive, porous bed in the bottom corners of the crucible. Most of this bed broke up into fine particles when the sodium was removed, but about 10% remained as pieces with one dimension larger than 1/2 in. These pieces had an average total void volume of 29% and an average void volume connected to the surface of 20%. The minimum value determined for any of the pieces examined were a total void volume of 20% and a connected void volume of 15%.

C. Experiment M3

The vessel pressure increased slowly during the first 200 msec after entry, after which the pressure sensors were struck by hot sodium and produced anomalous signals. The initial force on the crucible supports indicated that the UO_2 had not struck the bottom of the crucible, since the force increased slowly and with only a few small pulses. As in M1, the smooth force increase probably indicated a small difference in pressure between sections of the interaction vessel. After a 100-msec time following entry of the UO_2, the force first increased and then decreased within 80 msec by a series of irregular pulses perhaps caused by boiling sodium. During this period, the sodium pressure gradually increased to about 70 psia when, at 176 msec after entry, there was a sharp pressure pulse with a measured maximum pressure of 180 psia. This coincided with a sharp force pulse, but there was no detectable disturbance in the gas phase. There were five subsequent pulses in the sodium, the last occurring 720 msec after entry; all except the third was followed closely by an initial downward force and then a series of damped force oscillations having a frequency of 200 to 250 Hz. The rise time of the liquid-phase pressure pulses was less than 2 msec, which was the time resolution of the instrumentation in this run (the transducer signals were not recorded properly on magnetic tape). The rise times of the initial force pulses were measurable and were about 2 msec. As shown in Table II, the measured peak pressure of each pulse had no correlation with the measured peak force, but the impulses of these pressure signals could not be measured because of the poor time resolution.

D. Particle Size

The size distributions of UO_2 particles recovered from inside and outside the crucible after each experiment are shown in Fig. 7 and are compared with the size ranges of UO_2 particles recovered from TREAT tests and from small-scale laboratory experiments. (The dashed lines delineate this size range; test S3 produced the coarsest particles and E2 the finest.) The large pieces of UO_2 found in the crucible following M2 were not included in the size distributions. Samples of a few size fractions of particles recovered from the crucible after runs M2 and M3 were analyzed for molybdenum to determine the relative amounts of metal and oxide, and the results are shown in Table III. Other analyses had shown that chromium had volatilized almost completely during the thermite reaction.

Metal particles were concentrated in the coarser size fractions. A rough separation of sizes of metal and oxide particles was made by estimating the molybdenum content of the unanalyzed size fractions from a log-log plot of the measured molybdenum concentration against the average particle size with the constraint that the overall molybdenum content was

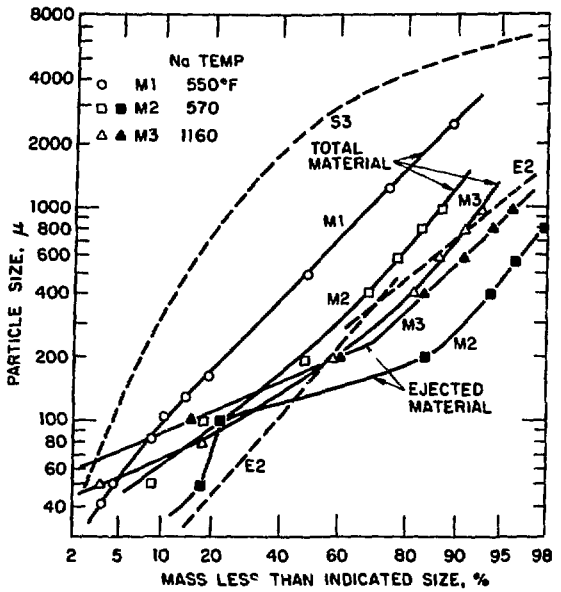

Fig. 7.
Size Distributions of Particulate Debris from Large-scale UO_2-Na Interactions (M Tests) (Compared to size range for in-pile tests, S3 and E2).

the stoichiometric value of 16.5 wt%. The particle-size distributions of the separate metal and oxide particles in the crucible after M2 and M3 are shown in Table III and Fig. 8. The metal particles were considerably coarser than the oxide particles, as would be expected from considerations of the stresses on liquid drops of metal and oxide quenched in sodium.[8] Armstrong[4] also found that molten UO_2 quenched in sodium formed finer particles than a molten metal (stainless steel).

The material ejected from the crucible in M2 appeared to be different than the material not ejected, because the ejected particles were considerably finer, and consisted primarily of particles between 100 and 200 μ and less than 50 μ. The molybdenum content of the 100- to 200-μ size fraction of the ejected material was 7.4 wt% compared to 8.3 wt% in similarly sized particles found in the crucible. Since the estimated precision of the sampling-analytical procedures was ±10% (2σ), this difference was probably not significant, and thus the difference between ejected and nonejected particles was only one of size. The segregation by size in M2 may have been due to the collection of molten UO_2 on the crucible bottom and the consequent poor dispersal of UO_2 particles in the bulk sodium. In M3, there was no evidence of a discrete layer of UO_2, and the ejected particles had nearly the same particle-size distribution as those not ejected.

In all three runs, the particles were primarily angular and irregularly shaped; probably less than 1% of the material was recovered as smooth, more-or-less spherical particles. Photographs of representative particles are shown in Fig. 9.

Table III. Particle-size Distributions from Molten-fuel Interaction Tests

Particle-size Range (μm)	Total Material within Range (wt frac)	Mo Content* (wt%)	Metal Particles** within Range (wt frac)	UO_2 Particles** within Range (wt frac)
		Run M2		
>1000	0.127		0.43	0.07
840-1000	0.036		0.06	0.03
595-840	0.059	21.1	0.08	0.06
420-595	0.078		0.08	0.08
210-420	0.209		0.16	0.22
105-210	0.311	8.3	0.15	0.34
53-105	0.089		0.03	0.10
<53	0.090	2.2	0.01	0.10
		Run M3		
>1000	0.093		0.22	0.07
840-1000	0.020		0.06	0.01
595-840	0.035	58.6	0.09	0.02
420-595	0.057		0.10	0.05
210-420	0.263		0.30	0.26
105-210	0.309	8.8	0.16	0.34
53-105	0.170		0.06	0.19
<53	0.052	2.6	0.01	0.06

*Colorimetric chemical analysis. Estimated standard deviation ±5%.

**Calculated and normalized size distributions assuming separate metal and oxide particles.

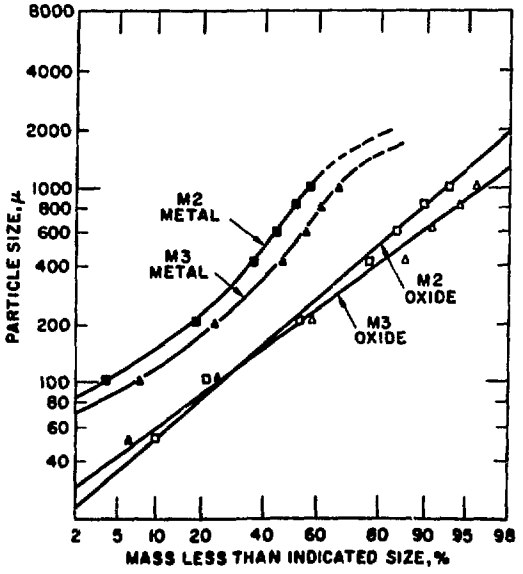

Fig. 8.
Size Distributions of Metal and Oxide Particulate Debris in Tests M2 and M3 (material remaining in crucible).

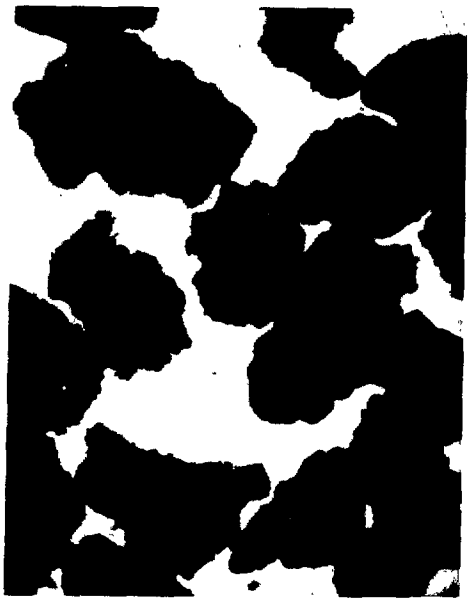

RUN #	M2
PARTICLE SIZE	-595, +420 μ
MAGNIFICATION	∿35X

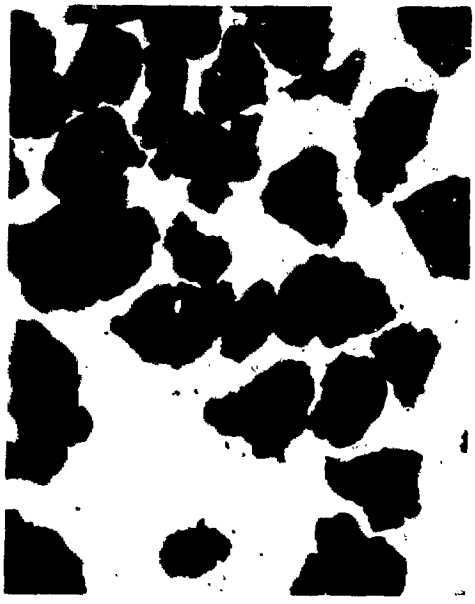

	M2
	-420, +210 μ
	∿35X

RUN #	M2
PARTICLE SIZE	-210, +105 μ
MAGNIFICATION	65X

	M1
	-44 μ
	160X

Fig. 9. Photographs of Particles Recovered from Large-scale Interactions

V. DISCUSSION OF RESULTS

Large-scale versions of the small-scale vapor explosions described by Armstrong,[6] were not observed in the three interaction experiments. The observed interaction events can be described qualitatively as rapid heating with some boiling of sodium and with perhaps a few isolated short-rise-time events occurring in the liquid phase. Because the magnitude and impulse of the sharp pressure pulses were in the same range as the pulses obtained by Armstrong[4] with a single drop of UO_2 weighing at most a few grams, it was assumed that the pulses observed in the large-scale tests were caused also by local interactions involving only a few grams of UO_2. Except for the very small energy content of these sharp pressure pulses, the heat available in the molten UO_2-Mo mixture was transferred rather slowly to sodium with a significant fraction of the heat producing sodium vapor. Most of the work potential of the interaction appeared as vapor at an elevated pressure, with a negligible fraction as kinetic energy of expelled liquid sodium.

A. Heat-transfer Rates

Instantaneous rates of heat transfer from the UO_2 were estimated from the rate of vapor production. The latter rate was calculated from the measured increase in the vessel pressure, assuming that the heat loss to the vessel atmosphere and condensation negligible for small time intervals immediately after entry of the UO_2 into the sodium. The sodium vapor was assumed to be produced at the instantaneous interface temperature between the UO_2 and sodium. That portion of the transferred heat that only heated liquid would not be determined by this procedure. However, the fraction of heat producing vapor would be expected to be highest immediately following entry, when the maximum heat-transfer rates shown in Table IV were calculated.

Table IV. Boiling Heat-transfer Rates

Run #	M1	M2	M3
Initial Sodium Temperature (°F)	550	570	1160
Calculated Instantaneous Interface Temperature (°F)	2150	2160	2570
Measured Maximum Heat-transfer Rate (to vapor production) $\frac{\text{Btu}}{(\text{hr})(\text{lb } UO_2)}$	2.4×10^6	1.7×10^6	0.28×10^6
Calculated Maximum Heat-transfer Rate $\frac{\text{Btu}}{(\text{hr})(\text{lb } UO_2)}$	25×10^6	29×10^6	26×10^6
Fraction of Available Heat to Sodium Vapor	0.21	0.25	0.13

The total amount of sodium vapor generated in the three runs was estimated from an overall heat balance for the sodium-containing crucible. The final temperature of the crucible and its contents was determined in M1 and M3 by thermocouples attached to the outside of the crucible, and in M2 by a thermocouple inserted in the melt a few seconds after the interaction. It was also assumed that the temperature of the sodium and UO_2 ejected from the crucible in runs M2 and M3 was the initial sodium temperature. As shown in Table IV, an upper limit to the fraction of the total available heat in the UO_2 that produced sodium vapor was about 0.25. Trends with experimental conditions are not significant because of inaccuracies in the calculations and measurements. A second value of 0.1 for M1 was obtained by an independent calculation based on the amount of sodium vapor required to raise the vessel pressure to 63 psia, the maximum recorded.

For runs M1 and M2, the maximum calculated boiling rates per pound of UO_2 were similar with the difference attributable to poorer contact between the fluids in M2, where the UO_2 struck the crucible bottom and flowed to the bottom corners before solidifying. Further indication of poor mixing in M2 was inferred from the shape of the pressure curves. The maximum rate of pressure rise occurred in M1 within a few milliseconds after entry; in M2, however, the maximum rate was delayed about 100 msec after entry.

In M3, the measurements made before the last pressure transducer failed about 200 msec after entry showed the pressure increasing slowly at a nearly linear rate and a maximum heat-transfer rate that was lower by an order of magnitude than in M1 or M2. This difference in heat rate, which was felt to be significant despite the early failure of the pressure sensors, was attributed to the interference between the vapor bubbles formed by adjacent hot oxide particles in the boiling pool. The volume of vapor formed in M3 may have been larger than in the two previous runs because the initial sodium temperature was higher and the initial vessel pressure was lower. Although the hot UO_2 particles may have been partially vapor blanketed, film boiling in the usual sense of film boiling at a single boundary could not have taken place at the sodium-UO_2 interface. A correlation of minimum film boiling temperature proposed by Henry,[9] which accounts for effects of subcooled liquid and low conductivity of the heat source, predicts that the bulk UO_2 temperature must be above 8000°F to support film boiling in sodium at 1160°F and 26 psia. Another indication that film boiling did not take place in M3 was that the UO_2 particles were not coarser, but were actually somewhat finer than particles produced in cooler sodium. For molten tin injected into water, Cho, Armstrong, and Gunther[10] found that as the tin temperature was increased, the metal particles became finer up to a point and then became coarser with a further temperature increase. Henry[9] has shown that the lowest temperature producing coarse particles corresponded to the minimum tin temperature required to support film boiling in this system.

It is of interest to compare the measured rates of heat transfer from the UO_2 to the sodium with calculated maximum rates similar to those used by Cho[11,12] to calculate the pressure effects resulting from the injection of molten fuel into sodium in large pools or in narrow channels. By neglecting the resistance to heat transfer in the sodium and characterizing the conduction in the UO_2 by a surface coefficient equal to the oxide

conductivity divided by the particle radius, heat fluxes were obtained that would appear to be in excess of the critical heat flux of boiling sodium for small particles. Although there are no experimental measurements of critical heat fluxes into subcooled, flowing sodium which characterize the situation in the interaction crucible, values in the range from 1 to 2 x 10^6 Btu/hr-ft^2 seem reasonable based on a few measurements with boiling pools of saturated sodium.[13] The calculated maximum heat flux from the UO_2 particles shown in Table IV was based on the total surface area of the material recovered after the interaction. Up to an arbitrary maximum of 1.3 x 10^6 Btu/hr-ft^2, the heat flux was calculated by

$$q = h(t_u - t_i),$$

where

t_u = temperature of UO_2 = 5680°F;

t_i = instantaneous interface temperature between UO_2 and sodium;

$h = 2K_u/D_p$;

K_u = thermal conductivity of UO_2 = 1.21 Btu/hr-ft-°F;

D_p = particle diameter.

The instantaneous interface temperature, which is also listed in Table IV, was estimated by

$$\frac{t_i - t_n}{t_u - t_i} = \left[\frac{K_u \rho_u \left(C_u + \frac{\Delta H_u}{t_u - t_i} \right)}{K_n \rho_n C_n} \right]^{\frac{1}{2}},$$

where

t_n = initial sodium temperature;

t_u = initial UO_2 temperature;

ρ = density;

C = heat capacity;

ΔH_u = heat of fusion of UO_2.

For the range of initial sodium temperature for the three runs, the limiting heat flux was reached for particles smaller than approximately 0.8 in. (2000 μ), which included most of the recovered particles.

Based on the surface area of the recovered UO_2 particles, the calculated ideal rates were higher by a factor of at least 10 than the highest

measured value. Mixing and contacting of the phases and interference effects between particles would influence the rate, and some indication of this was shown by the small difference in heat rates between M1, which seemed to have "good" mixing, and M2, which had poorer mixing. If the assumption of a critical boiling heat flux reasonably described the initial heat-transfer process, the high calculated heat rates suggested that a transfer area based on the sizes of the recovered particles was incorrect and that the interface area during the initial contacting was smaller by a factor of 10 to 100. The large majority of all particles recovered from these experiments was angular, and very few particles had smooth surfaces. Thus, it seemed likely that the final particles were not formed directly from quenching molten drops, but resulted from breaking of larger solid or partially solidified particles, perhaps because of thermal shock. Fragmentation of the liquid drops upon striking the surface of the sodium may have contributed to the dispersion of the UO_2, but this effect cannot be evaluated from these experiments since the size of drops approaching the surface could only be estimated.

The duration of the interaction events was of the order of 1 sec, as judged by the occurrence of sharp pressure pulses 0.45 sec after entry in M2 and 0.72 sec in M3. These pulses were evidence that hot UO_2 was still present at these times and was being exposed to sodium, perhaps by the shattering of large UO_2 particles having a frozen outer layer. Therefore, it is also suggested that for the geometry of these experiments - massive UO_2 and large unrestrained sodium pool - the fragmentation process was relatively slow, occurring on a time scale of roughly 1 sec. This time scale is very different from the fragmentation times of a few milliseconds used to represent the pressure pulses observed in TREAT tests simulating fuel melting in the coolant channels.[11] Despite the difference in the initial geometry and the apparent difference in the rate of fragmentation, the final sizes of particles recovered from the large-scale interactions were generally similar to the size range of particles from TREAT tests and from small-scale laboratory tests. These experiments demonstrated that large amounts of UO_2 will be fragmented extensively and will form a loose, porous debris bed. Even when the UO_2 struck the bottom of the crucible, over 90% of the UO_2 was dispersed and the rest formed a porous structure filled with sodium.

Experiment M1 supports the hypothesis that in a system with a high ratio of sodium to UO_2 the maximum pressure of sodium vapor produced would be the sodium vapor pressure at the instantaneous interface temperature. As shown in Fig. 4, the maximum vessel pressure recorded was 63 psia and the sodium vapor pressure at the calculated sodium-UO_2 interface temperature was 62 psia. In M2, for which the initial sodium temperature was similar to M1, the maximum vessel pressure was 105 psia and was limited by the venting of gases through the opened vessel cover. This higher pressure was not necessarily inconsistent with the conclusion from M1, because the pressure did not exceed 65 psia for at least 100 msec after entry, by which time the bulk sodium temperature must have risen considerably, while some molten UO_2 still may have been present. A thermocouple that was inserted in the crucible soon after the interaction showed a sodium temperature of 1300°F. However, in run M3, the calculated interface temperature was 2570°F, corresponding to a vapor pressure of 550 psia. Although pressure transducers failed early in this run, the vessel pressure did not exceed

100 psia because the vessel cover plate did not open. Heat losses and condensation may have been able to limit the pressure rise due to the low boiling rate.

B. Modeling Calculations

The FCI Parametric Model[11,12] was used to calculate liquid-phase pressures and sodium-slug velocities with input conditions to simulate M2. The input parameters for six cases, the calculated peak pressures, times of occurrence of these pressure peaks, and the times required for the sodium slug to be ejected from the crucible (travel 16.3 cm) are shown in Table V. Calculated data for four cases are shown in Figs. 10 to 13 as a function of time after the start of interaction.

Table V. FCI Calculations with Parametric Model

General Input Parameters	Oxide	Sodium
Total Mass (g)	3080	3230
Initial Temperature (°C)	3140	300
Injection Time (msec)	20	
UO_2/Sodium Wt Ratio in Interaction Zone		12.5
Depth of Interaction Zone (cm)		1.0
Initial Pressure (atm)		3.81
Restraining Sodium Column:		
Mass (g)		4650
Diameter (cm)		20.3
Depth (cm)		16.3

Summary of Calculations

	Additional Input Parameters				Results		
Case	Model	Restraint	Mixing or Fragmentation Time (msec)	Oxide-particle Radius (cm)	Peak Pressures (atm)	Time of Peak Pressures (msec)	Time of Sodium-slug Ejection (msec)
I	Mixing	Inertial	20	0.011	27	4.0	7.0
II	Fragmenting	Inertial	10	0.011	15 215 68	0.03 2.37 4.5	6.0
III	Fragmenting	Acoustic-inertial	10	0.011	13 152 69	0.135 2.50 4.5	6.0
IV	Fragmenting	Acoustic-inertial	0	0.011	3800 580	0.004 0.135	1.1
V	Quasi-steady State	Acoustic-inertial	-	0.06 and 0.121	Sodium slug does not lift within 4 msec[1] gentle boiling		
VI	Mixing	Inertial	20	0.121	Interaction zone cools off[2]		

(1) Initial sodium temperatures of 300 and 625°C.

(2) Sodium temperature in interaction zone assumed to be 1050°C after 2.0 msec.

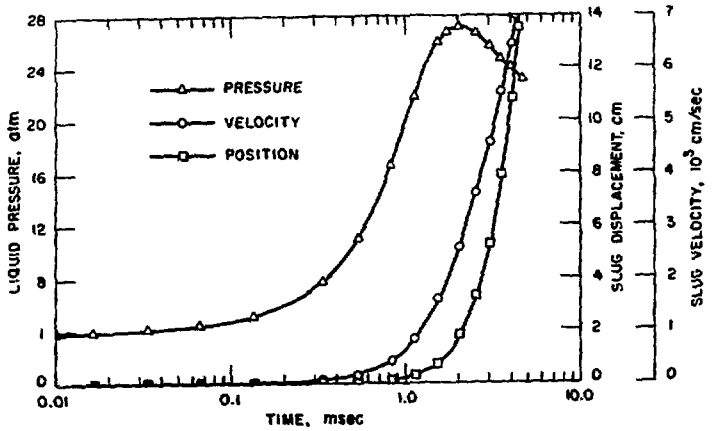

Fig. 10. Calculated Interaction Events for Case I.

Model: Mixing (mixing time 20 msec)
Restraint: Inertial

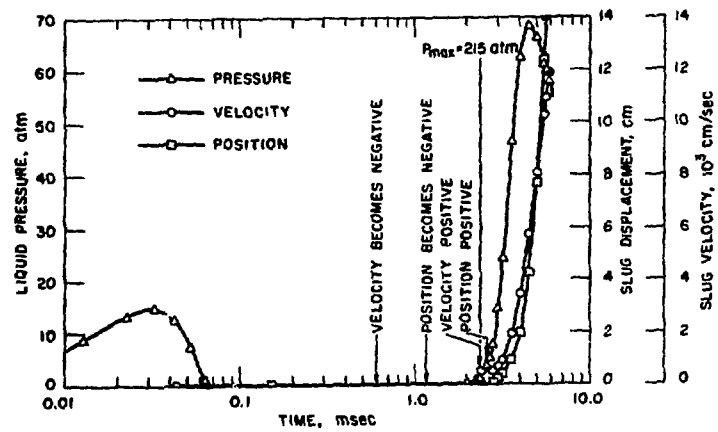

Fig. 11. Calculated Interaction Events for Case II.

Model: Fragmenting (fragmentation time 10 msec)
Restraint: Inertial

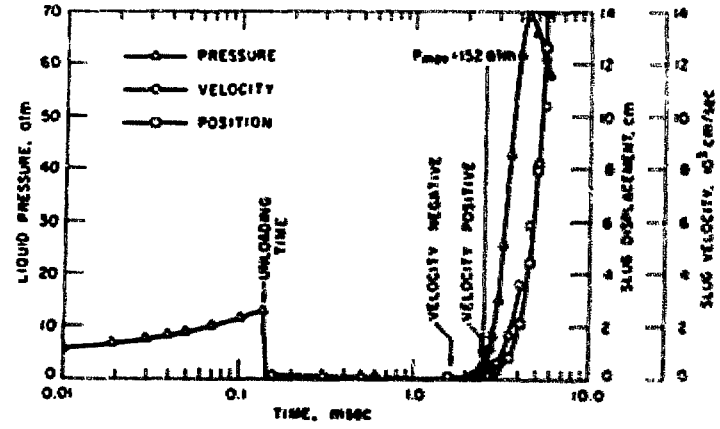

Fig. 12. Calculated Interaction Events for Case III.

Model: Fragmenting (fragmentation time 10 msec)
Restraint: Acoustic-inertial

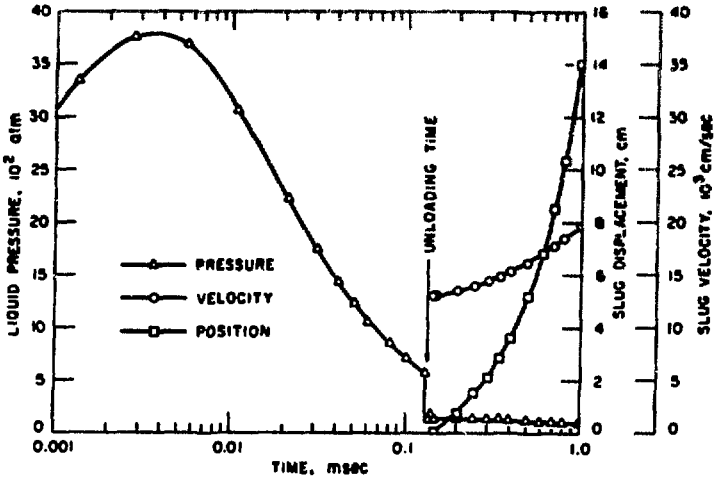

Fig. 13. Calculated Interaction Events for Case IV.

Model: Fragmenting (fragmentation time 0 msec)
Restraint: Acoustic-inertial

The "Mixing Model" assumed that oxide and sodium were added to an interaction zone at constant rates over a mixing time (20 msec in these calculations). The rate of heat transfer from UO_2 to sodium was represented by

$$\frac{dQ}{dt} = hA(t_u - t_n),$$

where

$h = K_u/R_u$;

K_u = thermal conductivity of UO_2 (= 0.005 cal/cm-sec-°C);

R_u = radius of UO_2 particles;

A = surface area of spherical UO_2 particles;

t_u = temperature of UO_2;

t_n = sodium temperature.

To obtain stable computer solutions for this case, it was necessary to assume an initial mixing time of 2 msec, during which the initially subcooled sodium in the interaction zone was heated to the saturation temperature corresponding to the initial pressure. The "Quasi-steady-state Model" assumed that initially all of the UO_2 was completely fragmented and dispersed in the sodium. It employed a similar formulation for the heat-transfer rate as the "Mixing Model." In the "Fragmentation Model," all of the oxide and sodium were initially mixed, and both the surface area and heat-transfer coefficient varied with time. The UO_2 surface area increased with time as

$$A(\theta) = A\left(1 - e^{-\theta/\theta_m}\right),$$

where

$A(\theta)$ = oxide surface area at time θ;

A = final surface area;

θ_m = fragmentation time constant.

The heat-transfer coefficient is given by

$$h = \frac{K_u}{\sqrt{\pi \alpha_u \theta}} + \frac{K_u}{R_u},$$

where

α_u = thermal diffusivity of oxide (= 0.0046 cm^2/sec).

In all cases the restraints on the expansion of the sodium in the interaction zone were inertia and weight of the sodium slug. This slug included one-half of the sodium and oxide in the mixing zone, and the slug length was taken as the length of an equivalent volume of sodium. Where an acoustic-inertial restraint was used in the calculations, the sodium slug did not move for times shorter than the acoustic unloading time for the initial pressure pulse created by liquid expansion. This time was twice the slug length divided by the sonic velocity (0.135 msec in all cases).

The first four cases calculated used a particle radius equal to the mass average radius of the particles recovered from M2. The Mixing Model (Case I) predicted a peak liquid-phase pressure of 27 atm and the complete ejection of the sodium slug from the crucible (when the slug had risen 16.3 cm) after 4.6 msec. For Cases II and III, using the fragmentation model without and with acoustic restraint, similar events were calculated. The initial pressure pulse due to liquid expansion caused a slight upward movement of the sodium slug, which relieved the pressure in the interaction zone. The falling slug compressed the heating liquid, resulting in a sharp pressure pulse that was followed by a gradually rising pressure from the boiling liquid and ejection of the sodium slug. A sharp and very large initial pressure pulse was calculated in Case IV because instantaneous dispersion and fragmentation was assumed, coupled with the high initial heat-transfer coefficient (caused by the $1/\sqrt{t}$ term in the expression for the heat-transfer coefficient). Therefore, at unloading time, the sodium slug had a very high velocity, and it was ejected from the crucible within 1.05 msec.

The liquid-phase pressures calculated for Cases I through IV did not correspond to events observed in the experiments. The calculated pressures were too large and occurred too soon after entry of UO_2 into the sodium, because the calculated rates of heat transfer to sodium were at least larger by an order of magnitude than the experimentally observed rates.

In Cases V and VI, the maximum overall heat-transfer rates as measured in M1 and M2 of roughly 1×10^6 cal/sec were represented in the calculations by assuming particle radii of 0.06 and 0.121 cm. For these low heat-transfer rates, the quasi-steady-state model showed, as expected, no boiling within 2 msec for sodium with an initial temperature of 300°C and only "gentle" boiling after 1 msec with an initial temperature of 625°C. The mixing model indicated that the heat-transfer rate was too slow to maintain the temperature of the sodium in the interaction zone, which was arbitrarily assumed to be 1050°C 2 msec after the start of the event.

The gas-phase shock pressures caused by the liquid-phase pressure pulses calculated in Cases I to IV and the sharp pressure pulses observed in M2 and M3 were estimated by

$$P_a = P_n\left[\frac{\rho_a C_a}{\rho_n C_n}\right],$$

where

P = pressure;

ρ = density;

C = sonic velocity;

(subscripts a and n refer respectively to argon gas and sodium liquid).

The calculated gas-phase shock pressures are shown in Table VI. Since the sensitivity of the gas-phase pressure transducers was about 2 psi (0.14 atm), only the calculated pressure pulses generated in Cases II and IV would have been detectable. The fact that no such gas-phase pressure pulses were recorded indicates that no large liquid-phase pressure pulses were generated in the experiments.

Table VI. Calculated Gas-phase Shock Pressures Corresponding to Liquid-phase Pressure Pulses

Calc. Case or Expt. No.	Liquid Phase Pressure Pulse (atm)	Gas Phase Pressure Pulse (atm)
I	27	0.02
II	215	0.15
III	152	0.11
IV	3800 580	2.7 0.41
M2	30	0.02
M3	4.8 to 20	0.003 to 0.014

C. Sodium Pressure

Liquid-phase pressure pulses with short rise times, similar to that measured in M2, apparently occurred in each run, but only indirect evidence of their occurrence was obtained in runs M1 (force oscillations) and M3 (pressure pulses with unresolved rise times and force oscillations). Their cause could not be determined, but it was suggested that the pulses were shock waves originating from the collapse of vapor bubbles in the subcooled liquid sodium.[14] The work potential of the observed or inferred pulses was negligible. Since Armstrong[4] had observed similar pressure pulses of

comparable sizes with less than 20 g of molten UO_2, it can be postulated that the magnitudes of these pulses are independent of the quantity of UO_2.

Through use of the surface area of UO_2 particles recovered after the interaction experiments, high heat-transfer rates were predicted by the Parametric Model with large, sharp pressure pulses occurring soon after UO_2 entry and rapid movement of the restraining sodium column. When heat-transfer rates approximating the measured rates were employed in the calculations, no pressure pulses and no significant movement of the sodium column for times up to several milliseconds were predicted. The observed interactions were characterized by heat-transfer rates lower than predicted and a few isolated pressure pulses occurring more than 100 msec after the initial UO_2 entry. The calculational model assumed that there is a definite zone in which fuel and sodium are mixed and that the expansion of this mixing zone is restrained by a column of sodium acting as a solid piston. Perhaps a more realistic picture of the interaction experiments is the dispersion of UO_2 particles throughout the sodium pool, such that each UO_2 particle or group of particles is surrounded by an interaction layer of hot sodium liquid and vapor which, in turn, is surrounded by the cool bulk sodium. Vapor generated by adjacent interaction zones would tend to interfere with the transfer of heat to the bulk sodium, especially when the ratio of fuel to sodium is high or the sodium temperature is high.

D. Particulate Formation

An important result of the experiments is the demonstration of the tendency to form particulate debris. In experiments M1 and M3, all UO_2 was converted to particulate. In experiment M2, about 90% of the UO_2 was converted to particulate; the other 10% formed large porous pieces. The marked tendency to form particulate is demonstrated by the fact that so much of the UO_2 was converted to particulate even though the initial sodium depth was only about 4 in. This is shown in Table VII, where it is apparent that it requires an almost equal weight of fuel to sodium in a sodium depth of only 4 in. before not all of the fuel is converted to particulate. The average loading in g-UO_2/cm^2 of UO_2 over the surface area of the crucible is also listed in Table VII.

Table VII. Fraction of Fuel Forming Particulate on Contact with Sodium

Exp.	Quantity		Na Temp, °F	UO_2 Loading, g-UO_2/cm^2-crucible	Fraction Particulate
	Fuel, lb	Na, lb			
M1	1.4	6.6	555	2.0	1.0
M3	3.0	6.6	1160	4.2	1.0
M2	6.8	6.6	570	9.5	0.9

E. Applications

The experiments indicate that the short-rise-time pressure pulses created by massive molten-fuel-sodium interactions with high ratios of sodium to fuel have negligible work potential, and their magnitude does not increase with the amount of molten fuel. The largest potential for mechanical work is by means of the sodium vapor generated over a period of roughly 1 sec.

Under the conditions of the experiments, about 20% of the heat was effective in generating sodium vapor. Under similar conditions in a reactor environment, the potential for doing work on the surroundings can be estimated. It is necessary to postulate a thermodynamic process. However, the potential for sodium vapor to do work on its fluid surroundings depends upon a number of factors other than the rate of pressure increase. Some of these are the inertial pressure, the drag forces on the fluids, and the condensation rate of vapor.

The experimental results show the marked tendency of molten UO_2 to form particulate after passage through only a few inches of sodium. Particle-size distributions obtained under the conditions of the experiments were not significantly different from those obtained in prior small-scale tests and in TREAT tests. Also, the results indicate that the metallic component of the mixture forms larger particles than the UO_2 component, which is consistent with previous small-scale results.[4]

VI. SUGGESTIONS FOR FUTURE EXPERIMENTS

Additional experiments with thermite-produced UO_2 dropped into an open crucible containing molten sodium could add confirmation to the low work potential of the infrequent liquid-phase pressure pulses. Also, it would be of value to investigate the apparent decrease in heat-transfer rate with increase in sodium temperature. A repeat of Experiment M3 and a test with 1500°F sodium, which according to Henry's correlation would cause film boiling, are suggested. Modifications of the apparatus are necessary to insure the survival of the vessel-pressure sensors and to prevent the blockage of the transducer stand-off tube in the sodium-containing crucible. Improved measurements of the temperatures of the sodium and the crucible immediately following the interaction should be made to improve the accuracy of the determination of the amount of sodium vapor produced.

Interaction experiments in geometries more nearly similar to reactor situations might be of considerable value to accident analysis now that tests with an open crucible have shown that destructive pressures are not produced. Subsurface injections of molten UO_2 into sodium would more nearly simulate ejections of molten fuel from the core region into the coolant. Also, the release of UO_2 into sodium contained in a hydraulic mockup of the inlet region of subassemblies could demonstrate the behavior of molten fuel on contact with sodium in a region of restricted dimensions.

VII. ACKNOWLEDGMENTS

The authors wish to acknowledge the advice of D. Armstrong and L. Bova in designing the instrumentation, the ingenuity and work of P. Gregoire in assembling and testing the instruments, and the assistance of J. Wrobel and J. Heiberger during the experiments. We also wish to thank R. Henry and H. Fauske for helpful discussions and suggestions on the interpretation of the experimental observations, and D. Cho for his assistance in making calculations with the FCI Parametric Code.

VIII. REFERENCES

1. T. R. Johnson, L. Baker, Jr., and J. R. Pavlik, Large-scale Molten Fuel-Sodium Interaction Experiments, Proc. Fast Reactor Safety Meeting, USAEC-CONF 740401-P2 (1974), p. 883.

2. T. R. Johnson, Molten-fuel Interaction Tests, in Reactor Development Program Progress Report, February 1973, ANL-RDP-14, p. 9.37 (March 22, 1973).

3. J. C. Hesson, R. H. Sevy, and T. J. Marciniak, Postaccident Heat Removal in LMFBRs: In-vessel Considerations, ANL-7859 (Sept. 1971).

4. D. R. Armstrong, F. J. Testa, and D. Raridon, Interaction of Sodium with Molten UO_2 and Stainless Steel Using a Dropping Mode of Contact, ANL-7890 (Dec. 1971).

5. J. J. Barghusen, R. W. Wright, C. E. Miller, J. F. Boland, and R. W. Mouring, In-pile Tests, in LMFBR Nuclear Safety Program Annual Report, ANL-7800, p. 321 (1971).

6. R. P. Anderson and D. R. Armstrong, Laboratory Tests of Molten-Fuel-Coolant Interactions, Trans. ANS, 15(1), 313 (1972); see also Reactor Development Program Progress Report, ANL-RDP-2, p. 8.31 (Feb. 1972).

7. D. R. Pedersen, T. F. Cannon, and C. J. Roop, Meltdown Cup, in Reactor Development Program Progress Report, July 1973, ANL-RDP-18, p. 7.70 (Aug. 29, 1973).

8. A. W. Cronenberg, T. C. Chawla, and H. K. Fauske, A Thermal Stress Mechanism for the Fragmentation of Molten Reactor Materials on Contact with Coolant, Trans. ANS, 17, 351 (Nov. 1973).

9. R. E. Henry, "A Correlation for the Minimum Film Boiling Temperature," Fourteenth National Heat Transfer Conference, AIChE Preprint 14 (Aug. 1973).

10. D. H. Cho, D. R. Armstrong, and W. H. Gunther, Molten Material - Coolant Interactions, Trans. ANS, 13(1), 385 (June 1970).

11. D. H. Cho, R. O. Ivins, and R. W. Wright, A Rate-limited Model of Molten Fuel-coolant Interactions, Model Development and Preliminary Calculations, ANL-7919 (March 1972).

12. D. H. Cho, W. L. Chen, and R. W. Wright, A Parametric Study of Pressure Generation and Sodium Slug Energy from Molten-fuel-coolant Interactions, ANL-8105 (Aug. 1974).

13. R. C. Noyes and H. Lurie, "Boiling Sodium Heat Transfer," Proceedings of Third International Heat Transfer Conference, AIChE/ASME (Aug. 1966).

14. T. G. Theofanous, H. S. Isbin, and H. K. Fauske, Sodium Bubble Collapse and Pressure Generation, Trans. ANS, 12(2), 909 (Nov. 1969).